Inflammation in rat pregnancy inhibits spiral artery remodeling leading to fetal growth restriction and features of preeclampsia

Tiziana Cotechini, Maria Komisarenko, Arissa Sperou, Shannyn Macdonald-Goodfellow, Michael A. Adams, and Charles H. Graham

Department of Biomedical and Molecular Sciences, Queen's University, Kingston, Ontario, Canada K7L 3N6

Fetal growth restriction (FGR) and preeclampsia (PE) are often associated with abnormal maternal inflammation, deficient spiral artery (SA) remodeling, and altered uteroplacental perfusion. Here, we provide evidence of a novel mechanistic link between abnormal maternal inflammation and the development of FGR with features of PE. Using a model in which pregnant rats are administered low-dose lipopolysaccharide (LPS) on gestational days 13.5–16.5, we show that abnormal inflammation resulted in FGR mediated by tumor necrosis factor-α (TNF). Inflammation was also associated with deficient trophoblast invasion and SA remodeling, as well as with altered uteroplacental hemodynamics and placental nitrosative stress. Moreover, inflammation increased maternal mean arterial pressure (MAP) and was associated with renal structural alterations and proteinuria characteristic of PE. Finally, transdermal administration of the nitric oxide (NO) mimetic glyceryl trinitrate prevented altered uteroplacental perfusion, LPS-induced inflammation, placental nitrosative stress, renal structural and functional alterations, increase in MAP, and FGR. These findings demonstrate that maternal inflammation can lead to severe pregnancy complications via a mechanism that involves increased maternal levels of TNF. Our study provides a rationale for the use of antiinflammatory agents or NO-mimetics in the treatment and/or prevention of inflammation-associated pregnancy complications.

CORRESPONDENCE
Charles H. Graham:
grahamc@queensu.ca

Abbreviations used: CBC, complete blood cell count; EDV, end diastolic flow velocity; ET-1, endothelin-1; Eta, etanercept; FGR, fetal growth restriction; GBM, glomerular basement membrane; GD, gestational day; GTN, glyceryl trinitrate; MAP, mean arterial pressure; MT, mesometrial triangle; NHS, normal horse serum; NO, nitric oxide; PD, postnatal day; PE, preeclampsia; PSV, peak systolic flow velocity; RI, resistance index; RUPP, reduced uteroplacental perfusion; SA, spiral artery.

Preeclampsia (PE) is a serious condition that affects 3–10% of all pregnancies (Lyall and Belfort, 2007), and is characterized by the development of maternal hypertension (>140/90 mm Hg) and proteinuria (≥300 mg/24 h; Redman and Jefferies, 1988). PE usually develops after 20 wk of gestation, and is difficult to treat except by early delivery, which can result in neonatal complications. In addition to increasing the maternal and fetal risk of morbidity and mortality, the pathological processes associated with PE can restrict fetal growth and impair development. Fetal growth restriction (FGR) occurs when the fetus fails to achieve its genetically predetermined growth potential (Gardosi et al., 1992). It is the second leading cause of fetal death and is often associated with PE (Peleg et al., 1998; Vatten and Skjaerven, 2004).

Although the precise mechanisms leading to the development of FGR/PE remain unknown, there is evidence that these complications are associated with an aberrant maternal inflammatory response. Women afflicted by FGR/PE exhibit a heightened inflammatory state; proinflammatory cytokines and chemokines, such as TNF, IL-6, and MCP-1, are elevated systemically and locally in the placenta (Redman et al., 1999; Borzychowski et al., 2006; Jain et al., 2007; LaMarca et al., 2007; Szarka et al., 2010). This abnormal inflammatory response leads to oxidative and nitrosative stress associated with decreased nitric oxide (NO) bioavailability (Roggensack et al., 1999; Lowe, 2000; Borzychowski et al., 2006).

It is widely recognized that the placenta plays an important role in the pathophysiology of FGR/PE (Page, 1939; Koga et al., 2010). In the two-stage model of PE initially proposed by Redman (1991), deficient placental perfusion

The Rockefeller University Press $30.00
J. Exp. Med. 2014 Vol. 211 No. 1 165-179
www.jem.org/cgi/doi/10.1084/jem.20130295

The Journal of Experimental Medicine

(stage one) leads to the release of vasoactive factors that precipitate the onset of the maternal syndrome (stage two) (Roberts and Gammill, 2005). Placental perfusion is dependent on adequate remodeling of the uterine spiral arteries, a process whereby endovascular trophoblast cells invade and replace the endothelium and vascular smooth muscle of these vessels (Boyd and Hamilton, 1970). Hence, a deficiency in this remodeling process is thought to account for the poor placental perfusion associated with FGR/PE.

Despite the strong association between abnormal maternal inflammation and FGR/PE, it is not known whether inflammation is causally linked to the deficient spiral artery (SA) remodeling that characterizes these pregnancy complications. Reister et al. (1999) examined vessels from preeclamptic pregnancies and found that an increase in the distribution of macrophages around the spiral arteries was associated with impaired trophoblast invasion. Moreover, our in vitro studies revealed that activated macrophages inhibit trophoblast invasion by secreting TNF at subapoptotic levels (Renaud et al., 2005). Other studies have additionally described an inhibitory role of TNF in the regulation of trophoblast motility and migration (Todt et al., 1996; Renaud et al., 2007; Venegas-Pont et al., 2010). Using a rat model, we describe a novel mechanism by which abnormal maternal inflammation results in deficient SA remodeling and altered uteroplacental perfusion. Our study also reveals that this inflammation-induced deficiency in vascular adaptation is associated with FGR and features of PE.

RESULTS

LPS administration induces a systemic and local inflammatory response and results in TNF-mediated FGR

To assess whether LPS administration affects in utero growth, we defined FGR in our rats as a fetal weight falling below the 10th percentile for gestational age. To determine the threshold of FGR, we evaluated the distribution of all fetal weights from the saline-treated control cohort (n = 22 dams; n = 305 fetuses; mean fetal weight = 0.9244 ± 0.007 g); fetuses with weights <0.8071 g (lower 10th percentile) were designated as FGR (Fig. 1 A). Daily LPS administration on gestational day (GD) 13.5–16.5 significantly decreased fetal weight measured on GD 17.5 (n = 28 dams; n = 258 fetuses; mean fetal weight = 0.8421 ± 0.006 g; Fig. 1 A and Table 1). None of the rats treated with LPS experienced preterm birth. To determine

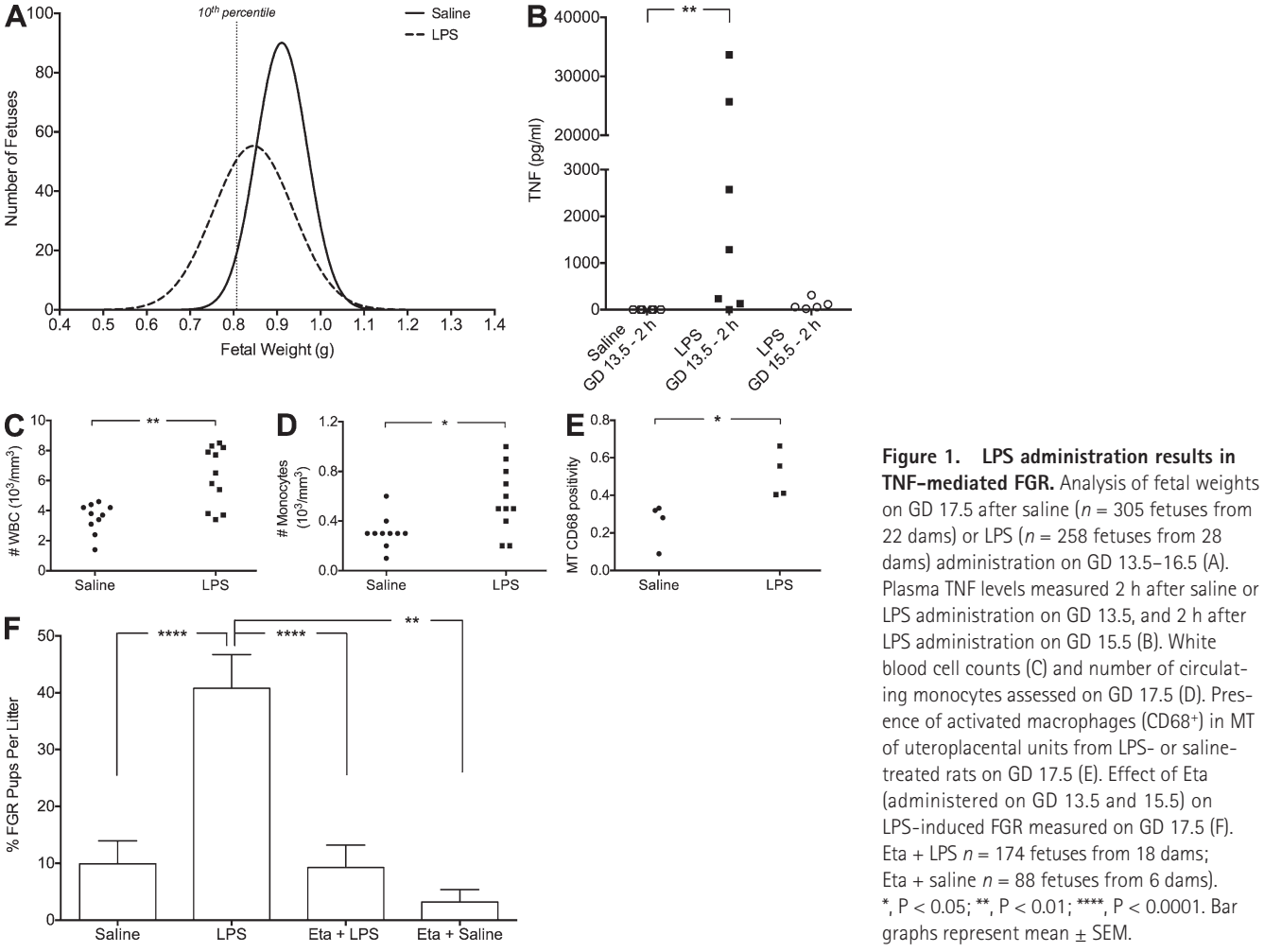

Figure 1. LPS administration results in TNF-mediated FGR. Analysis of fetal weights on GD 17.5 after saline (n = 305 fetuses from 22 dams) or LPS (n = 258 fetuses from 28 dams) administration on GD 13.5–16.5 (A). Plasma TNF levels measured 2 h after saline or LPS administration on GD 13.5, and 2 h after LPS administration on GD 15.5 (B). White blood cell counts (C) and number of circulating monocytes assessed on GD 17.5 (D). Presence of activated macrophages ($CD68^+$) in MT of uteroplacental units from LPS- or saline-treated rats on GD 17.5 (E). Effect of Eta (administered on GD 13.5 and 15.5) on LPS-induced FGR measured on GD 17.5 (F). Eta + LPS n = 174 fetuses from 18 dams; Eta + saline n = 88 fetuses from 6 dams). *, $P < 0.05$; **, $P < 0.01$; ****, $P < 0.0001$. Bar graphs represent mean ± SEM.

Table 1. Fetal weights assessed on GD 17.5

	Saline	LPS	Eta + LPS	GTN + LPS	Eta + Saline	GTN + Saline
Average FW[a] (g)	0.9244[c] (0.910–0.935)	0.8421 (0.831–0.854)	0.9284[c] (0.917–0.940)	0.8794[b] (0.866–0.893)	0.9192[c] (0.904–0.935)	0.8971[c] (0.882–0.912)
No. of dams	22	28	16	16	6	10
No. of fetuses	305	258	174	187	88	134

[a]Data are represented as mean (lower 95% confidence interval–upper 95% confidence interval). FW, fetal weight.
[b]$P < 0.001$ versus LPS.
[c]$P < 0.0001$ versus LPS.

whether LPS administration induced a maternal inflammatory response, we evaluated circulating plasma levels of TNF. As early as 2 h after the initial LPS injection (10 μg/kg), TNF levels were detectable and elevated compared with levels in saline-treated controls (Fig. 1 B and Table 2). On GD 15.5, 2 h after the third LPS injection, TNF levels were still detectable, though decreased, compared with GD 13.5 (Fig. 1 B). Importantly, white blood cell (WBC) counts performed on whole blood taken on GD 17.5 (24 h after the final LPS injection) were significantly elevated compared with WBC counts from blood of saline-treated control rats (Fig. 1 C and Table 2). Differential cell counts revealed increased numbers of circulating granulocytes (Table 2), lymphocytes (Table 2), and monocytes (Fig. 1 D and Table 2) contributing to the elevated WBC count in dams exposed to LPS. The presence of local uteroplacental macrophages in LPS-treated rats was revealed by immunohistochemistry against the lysosomal marker for activated macrophage CD68. On GD 17.5, CD68 immunostaining density was significantly higher in the mesometrial triangles (MTs) associated with growth-restricted fetuses from LPS-treated dams compared with normal-growth fetuses from saline-treated control dams (Fig. 1 E). Interestingly, LPS administration to nonpregnant animals revealed a pregnancy-specific effect: WBC counts in blood from nonpregnant LPS-treated animals were not significantly different from WBC counts in blood from saline-treated nonpregnant control animals (Table 2). Moreover, TNF levels measured 2 h after LPS (10 μg/kg) administration to nonpregnant animals were substantially lower than TNF levels measured from pregnant animals (Table 2).

To determine whether increased TNF levels are involved in the development of FGR, we administered the TNF inhibitor etanercept (Eta; 10 mg/kg; $n = 16$ dams; $n = 174$ fetuses) on GD 13.5 and 15.5, 6 h before injecting LPS. Compared with litters from LPS-treated animals, which exhibited a mean of ∼40% FGR (Fig. 1 F), treatment with Eta completely prevented LPS-induced FGR, indicating that TNF may be a key cytokine in the pathogenesis of inflammation-induced FGR (Fig. 1 F). The mean fetal weight from animals treated with Eta alone ($n = 6$ dams; $n = 88$ fetuses; mean fetal weight = 0.9192 ±

Table 2. Assessment of parameters of inflammation[a]

	Saline[b]	LPS[b]	Eta + LPS	GTN + LPS	NP Saline	NP LPS
No. of WBC[c]	3.52 (1.4–4.6)[h]	6.29 (3.4–8.5)	4.03 (1.3–5.8)[e]	3.06 (1.2–5.9)[h]	3.55 (2.5–4.8)[g]	2.23 (1.1–3)[h]
No. of monocytes[c]	0.31 (0.1–0.6)[e]	0.57 (0.2–1.0)	0.31 (0.1–0.5)[e]	0.25 (0.1–0.5)[g]	0.42 (0.2–0.6)	0.2 (0.1–0.3)[e]
No. of granulocytes[c]	2.2 (1.0–2.9)[h]	4.1 (2.2–5.7)	2.76 (0.9–3.9)[e]	2.06 (0.8–3.1)[h]	1.55 (1.4–1.8)[i]	1.2 (0.4–1.8)[i]
No. of lymphocytes[c]	1.01 (0.3–1.6)[f]	1.61 (0.7–2.6)	0.95 (0.3–1.4)[f]	0.75 (0.3–1.4)[e]	1.58 (0.9–2.7)	0.83 (0.4–0.9)[f]
No. of animals (CBC analysis)	10	11	8	8	6	4
No. animals (TNF analysis)	7	7	5	6	4	4
Plasma TNF (pg/ml)[d]	undetectable (0)	1285 (0–33643)[k]	2132 (0–8377.2)[j]	111.1 (0–127.3)	undetectable (0)	61.05 (0–240.8)

[a]WBC, white blood cells; NP, non-pregnant.
[b]Some data are represented in Fig. 1, B–D.
[c]CBCs were performed on GD 17.5, 24 h after the last LPS injection. Data are expressed as mean (range).
[d]Plasma was collected 2 h after saline/LPS administration to NP animals or 2 h after saline/LPS administration to pregnant animals on GD 13.5. Data are represented as median (range).
[e]$P < 0.1$ versus LPS.
[f]$P < 0.05$ versus LPS.
[g]$P < 0.01$ versus LPS.
[h]$P < 0.001$ versus LPS.
[i]$P < 0.0001$ versus LPS.
[j]$P < 0.05$ versus saline.
[k]$P < 0.01$ versus saline.

0.008 g) did not significantly differ from the mean fetal weight from saline-treated rats and did not result in significant FGR (Fig. 1 F and Table 1).

LPS-induced FGR is linked to deficient interstitial trophoblast invasion and impaired endovascular SA remodeling

Establishment and maintenance of adequate uteroplacental perfusion is necessary to support fetal growth and development. Because impaired trophoblast-mediated SA remodeling is often linked to FGR/PE, we examined whether abnormal maternal inflammation is associated with deficient vascular remodeling. Immunohistochemistry for cytokeratin (to identify trophoblasts) and α-actin (to identify smooth muscle) revealed evidence of trophoblast infiltration in the spiral arteries of all treatment groups (Fig. 2 A). However, the mean cross-sectional area of spiral arteries from uteroplacental units associated with LPS-induced FGR was significantly smaller than the cross-sectional area of vessels from uteroplacental units associated with normal fetal growth in saline-treated control rats (Fig. 2, A and B). Eta treatment prevented the LPS-induced reduction in mean SA cross-sectional area (Fig. 2, A and B).

Assessment of interstitial trophoblast invasion was examined using image analysis software. Specifically, the total area occupied by cytokeratin-positive trophoblast cells invading into the MT was expressed as a percentage of the total MT area (Fig. 2 C). LPS administration significantly decreased trophoblast invasion through a mechanism that may be dependent on TNF (Fig. 2 D). Moreover, the degree of interstitial trophoblast invasion was significantly and positively correlated with SA cross-sectional area across all treatment groups (Fig. 2 E).

LPS administration alters uteroplacental perfusion and is associated with placental nitrosative stress, whereas glyceryl trinitrate (GTN) prevents inflammation-induced FGR

The uteroplacental and fetoplacental vasculatures were visualized by ultrasound biomicroscopy (Fig. 3 A). At each of 3–4 implantation sites per animal, Doppler waveforms were recorded and analyzed offline by a blinded observer. The average SA resistance index (RI) from LPS-treated dams was significantly increased compared with control and Eta + LPS-treated animals (Fig. 3 B). This elevated SA RI in the LPS-treated cohort was negatively correlated with umbilical artery peak systolic flow velocity (PSV; Fig. 3 C). Across all treatment groups, SA RI was positively correlated with maternal channel RI (Fig. 3 D). These data, combined with evidence of nitrosative stress (measured by ELISA) in placentas from the

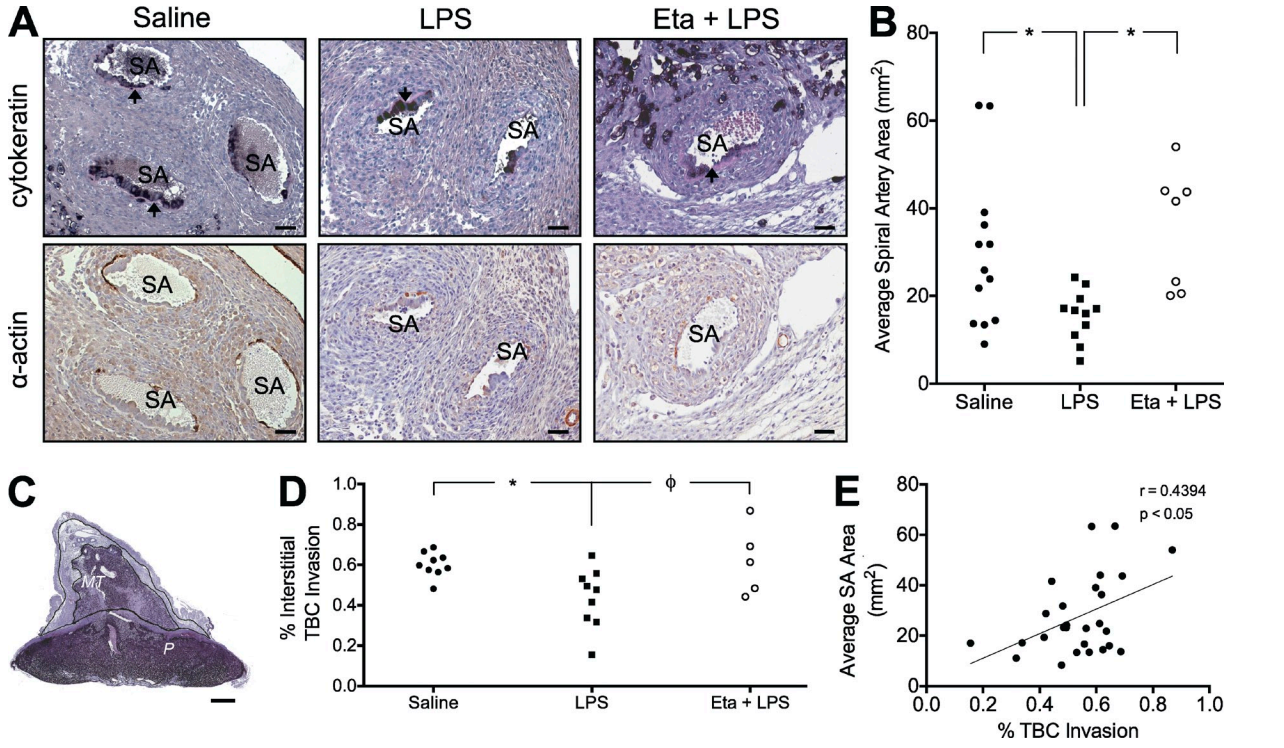

Figure 2. TNF is causally linked to deficient trophoblast invasion and SA remodeling associated with FGR. Spiral arteries from all treatment groups exhibited evidence of remodeling, including the presence of cytokeratin-positive endovascular trophoblast cells (black cells) resting on a fibrinoid layer (arrows) and the absence of α-actin⁺ (brown stain) smooth muscle (A). Effect of LPS administration on SA remodeling (A and B). Mean SA cross-sectional area in uteroplacental units (B). Interstitial trophoblast invasion into the MT was quantified as the percent area of the MT infiltrated by cytokeratin-positive trophoblast cells (C and D). Correlation of interstitial trophoblast invasion and mean spiral artery cross-sectional area for all treatment groups (E). *n* = 1–2 implantation sites for 5–9 animals/group; MT, mesometrial triangle; P, placenta; TBC, trophoblast cells. Φ, P = 0.0530; * P < 0.05. Bars: (A) 50 µm; (C) 1 mm.

LPS-treatment group (Fig. 3 E), indicate that inadequate SA perfusion has measurable downstream effects.

Given that NO acts as a vasodilator, we evaluated whether administration of the NO-mimetic GTN could prevent LPS-induced increases in SA RI, thereby improving perfusion and preventing FGR. Transdermal GTN administration (GD 12.5–17.5) to LPS-treated rats normalized SA RI and decreased the detection of placental nitrotyrosine (Fig. 3, B and E). Because several of the placentas analyzed from all treatment groups had levels of nitrotyrosine that fell below the detection limit of the assay, we could not correlate fetal weights to nitrotyrosine levels. Interestingly, we found that GTN administration also prevented the increase in maternal plasma TNF levels measured 2 h after the initial LPS injection on GD 13.5 (Table 2). These data support the concept that normalization of uteroplacental perfusion attenuates TNF release after LPS administration. Furthermore, compared with rats treated with LPS alone, rats that were additionally administered GTN exhibited significantly reduced WBC counts, including decreased circulating lymphocyte, monocyte, and granulocyte numbers by GD 17.5 (Table 2). Importantly, treatment with GTN prevented LPS-induced FGR (15.73% FGR offspring/litter ± 5.28% for rats treated with LPS + GTN compared with 40.78% FGR offspring/litter ± 5.60% for rats treated with LPS alone; $P < 0.01$). Treatment with GTN alone did not affect mean fetal weight (0.8942 ± 0.008 g; Table 1) and did not result in FGR (9.10% FGR offspring/litter ± 3.87%). Together, these results provide evidence that inflammation and FGR in LPS-treated rats are linked to inadequate uteroplacental perfusion.

LPS administration increases mean arterial pressure (MAP) through a mechanism dependent on TNF

MAP was assessed by radiotelemetry ($n = 5$ dams/group). To determine the effect of LPS on MAP, 24-h time point data were normalized to GD 11 (the GD before treatments were initiated). There was no difference in MAP profiles between any of the treatment groups from GD 0 to 11. Administration of LPS resulted in increased Δ MAP compared with saline-treated controls (Fig. 4 A). Eta treatment completely prevented the elevation in MAP associated with LPS administration (Fig. 4 A). Moreover, treatment with GTN partially attenuated

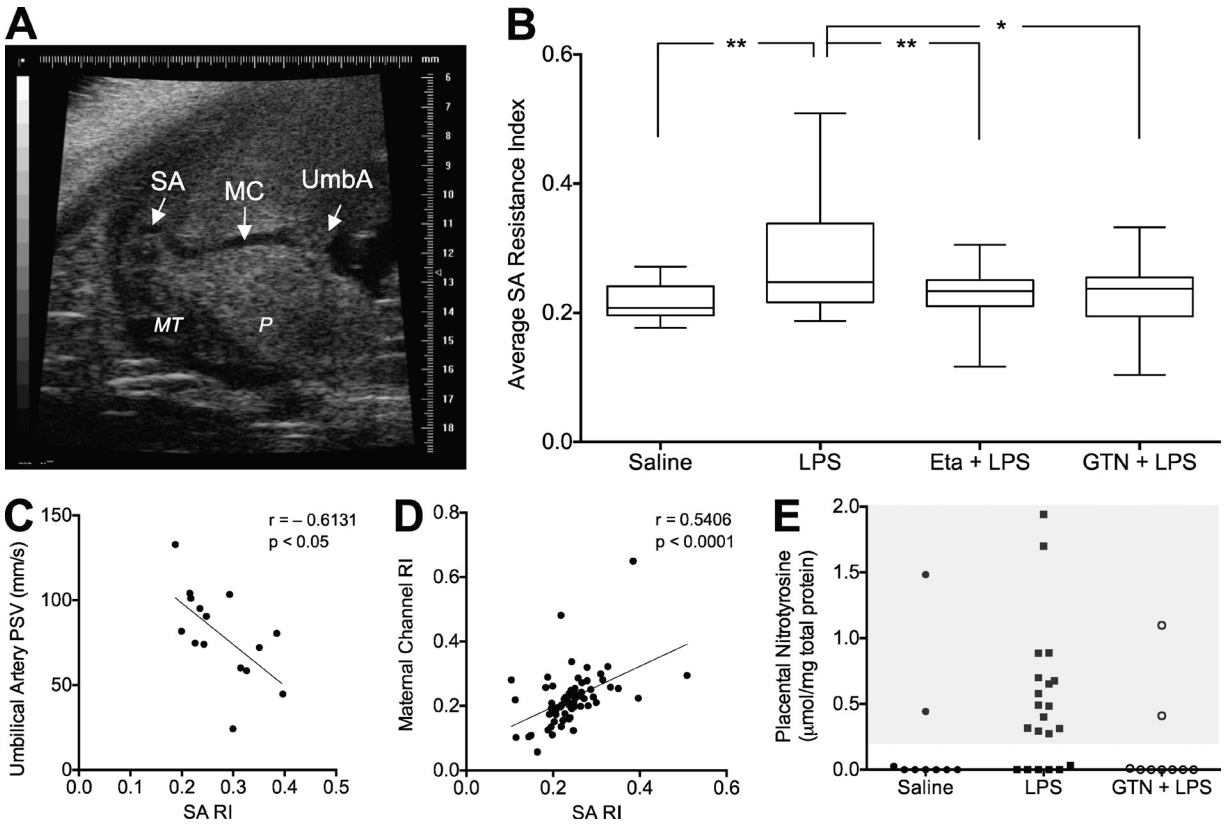

Figure 3. LPS-induced FGR is linked to uteroplacental hemodynamic alterations associated with nitrosative stress. Ultrasound biomicroscopy was used to visualize the vasculature within implantation sites, including spiral arteries, maternal channels, and the corresponding fetal umbilical artery (A). Mean SA RI measured from implantation sites (2–3 spiral arteries measured from 3–4 implantation sites per animal; $n = 6–7$ dams per group; B). Correlation of mean SA RI with the corresponding umbilical artery PSV from LPS-treated animals (C). Correlation of mean SA RI with the corresponding maternal channel RI across all treatment groups (D). Detectable nitrotyrosine (shaded box) in placentas from rats treated with saline, LPS, or LPS + GTN (E). *, $P < 0.05$; **, $P < 0.01$. UmbA, umbilical artery; MC, maternal channel; MT, mesometrial triangle; P, placenta; SA, spiral artery. Whiskers in B represent the 5th and 95th percentiles.

the LPS-induced alterations in MAP (Fig. 4 A). Whereas rats treated with saline, Eta + LPS, or GTN + LPS exhibited a progressive and significant decrease in MAP relative to baseline (GD 11) throughout the duration of the study, MAP from LPS-treated animals was significantly elevated on GD 13 and GD 14 and remained at baseline levels thereafter (Fig. 4 B). Compared with rats in all the other treatment groups, overall, MAP of rats treated with LPS alone was significantly elevated (Fig. 4 C).

To determine whether LPS affected fetal weight beyond GD 17.5, the pups born to dams instrumented with radiotelemetry transducers were weighed on postnatal day (PD) 1.5 and 7.5. Pups born to LPS-treated mothers were significantly smaller than those from all other treatment groups on PD 1.5 (Fig. 4 D); however, by PD 7.5 the weights of pups from LPS-treated animals were not significantly different from the weights of pups from saline-treated animals (Fig. 4 E). Eta and GTN administration normalized pup weight measured on PD 1.5, and by PD 7.5 pups born to Eta-treated mothers were significantly larger than pups from both saline-treated and LPS-treated animals (Fig. 4 E).

Nonpregnant rats (n = 4) were instrumented with radiotelemetry transducers to determine whether the effects of LPS on MAP are pregnancy specific. All animals were administered four saline injections, followed by four LPS injections with a 3-d rest period between treatments. Analysis revealed a significant elevation in MAP after the second LPS injection when compared against the second saline injection (Table 3).

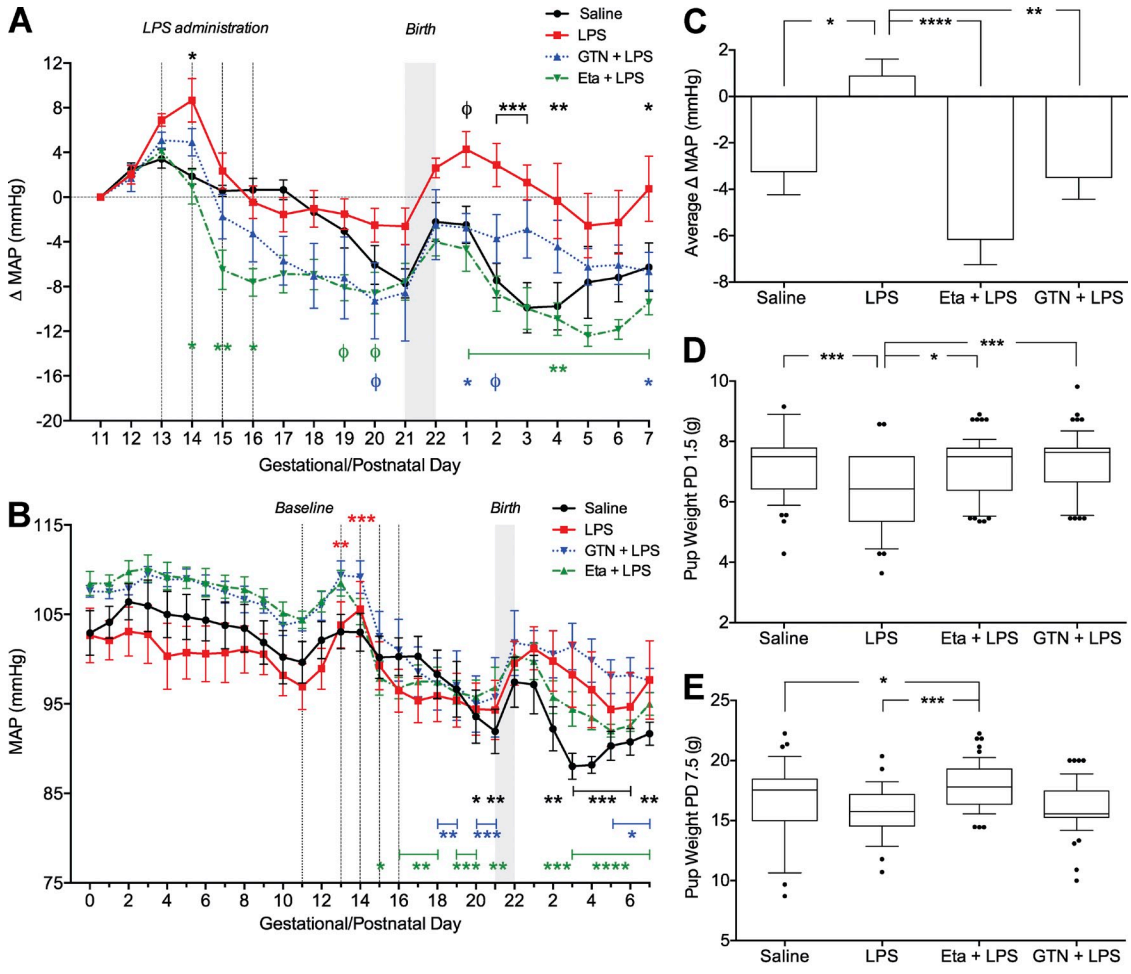

Figure 4. Elevated MAP is causally linked to increased maternal TNF levels and is associated with FGR at birth. To observe the treatment-specific effects on MAP, all animals were normalized to GD 11. Change in MAP corresponding to saline (n = 5 dams) or LPS (n = 5 dams) administration on GD 13.5–16.5 (dashed vertical lines) and Eta (n = 5) or GTN administration (n = 5) to LPS-treated animals (A). Full gestational MAP profiles (GD 0–PD 7) in rats from all treatment groups (n = 5 for each group; B). Mean overall change in MAP spanning GD 11–PD 7 in rats from all treatment groups (C). Weight of pups assessed on PD 1.5 (D) and 7.5 (E); saline, n = 45 pups; LPS, n = 35 pups; Eta + LPS, n = 56 pups; GTN + LPS, n = 53 pups. Φ, P < 0.1; *, P < 0.05; **, P < 0.01; ***, P < 0.001; ****, P < 0.0001. Symbols in A denote significant differences from LPS-treated animals; asterisks and asterisks within brackets in B denote significant differences at each day compared with baseline (GD 11); shaded regions in A and B represent the day of birth for all dams; points in A and C represent mean ± SEM; points in B represent 24-h mean MAP ± SEM; whiskers in D and E represent the 10th and 90th percentiles.

However, this LPS-induced increase in MAP in nonpregnant rats was of a lower magnitude (∼3.7 mmHg) than the increase in blood pressure observed in pregnant rats after the second LPS injection (∼8.7 mmHg).

LPS administration induces renal alterations and proteinuria associated with alterations in MAP

Maternal kidneys harvested on GD 17.5 were analyzed and the degree of glomerular pathology was assessed by a blinded observer using a scoring system (0–4; 0, no pathology; 4, severe pathology). Glomeruli from LPS-treated dams exhibited mesangial hypercellularity and occlusion of capillary loops and the urinary space (Fig. 5 A) resulting in a significantly higher histopathological score (Fig. 5 B). Ultrastructural analysis revealed a significant thickening of the glomerular basement membrane (GBM; Fig. 5 C). Treatment with Eta prevented the LPS-induced renal histopathological alterations and trended ($P = 0.0562$) toward preventing the thickening of the GBM (Fig. 5, A–C). Treatment with GTN was most effective at preventing the LPS-induced renal pathologies associated with inflammation-induced FGR (Fig. 5, A–C). Glomeruli from nonpregnant animals ($n = 4$) receiving the same schedule of LPS injections did not show signs of renal pathology and were not different from glomeruli of control animals (unpublished data). These results indicate that the effects of LPS on renal alterations are pregnancy specific.

To determine whether structural renal alterations were associated with functional and measurable changes, proteinuria (total protein/creatinine) was assessed in urine collected from the animals instrumented with radiotelemetry transducers. In the LPS-treatment group, changes in the protein/creatinine ratios calculated from baseline (mean protein/creatinine on GD 10.5–12.5) trended to correlate positively with changes in MAP ($P = 0.0536$; Fig. 5 D). A correlation between the change in MAP and the change in urine protein/creatinine ratios was not observed with any other treatment group. Overall, LPS administration significantly elevated the protein/creatinine ratio and this effect was prevented with GTN or Eta treatment (Fig. 5 E).

DISCUSSION

The main novel findings of this study are that abnormal maternal inflammation impairs SA remodeling, alters uteroplacental perfusion, and leads to FGR associated with some features of PE in a rat model. Our findings also reveal that the effects of maternal inflammation on the deficient vascular remodeling and altered uteroplacental perfusion associated with FGR/PE are largely mediated by TNF.

Circulating TNF levels are increased in a large proportion of women with FGR/PE (Conrad et al., 1998; Germain et al., 2007; Peraçoli et al., 2007; Zhou et al., 2012). Interestingly, TNF levels were reported to be significantly higher in preeclamptic pregnancies complicated by FGR compared with those with normal fetal growth in the third trimester (Tosun et al., 2010). Moreover, levels of TNF, and its stable soluble receptor p55, were increased early in pregnancies subsequently complicated by PE (Hamai et al., 1997; Williams et al., 1998). In our model, maternal TNF levels increased substantially within 2 h of LPS administration on GD 13.5 and remained detectable after three subsequent injections of LPS by GD 15.5. The diminished TNF response to LPS on GD 15.5 is likely the result of tolerance. A similar phenomenon occurring after repeated LPS exposure has been previously described (Faas et al., 2004). Nevertheless, despite attenuated TNF levels after subsequent injections of LPS, immune maladaptation persisted at least up to GD 17.5, as indicated by results showing increased circulating numbers of lymphocytes, granulocytes and monocytes, as well as high numbers of CD68-positive activated macrophage cells in the MTs of FGR uteroplacental units at this GD. Monocytes and activated macrophages are primarily responsible for TNF release (Hunt, 1989; Renaud et al., 2005) and have been localized in greater proportions around inadequately remodeled spiral arteries from preeclamptic pregnancies (Reister et al., 2001).

In addition to exerting systemic effects on cell survival, vascular permeability, neutrophil activation, and various cytokine cascades, TNF has also been shown to interact with the TNF receptor-1 present on invasive extravillous trophoblasts (Knöfler et al., 1998; Renaud et al., 2009). Previous work from our laboratory described the TNF-mediated release of monocyte chemoattractants from extravillous trophoblasts, which may further amplify the proinflammatory cascade (Renaud et al., 2009). We and others have also shown that macrophage-derived TNF inhibits trophoblast invasion in vitro (Bauer et al., 2004; Renaud et al., 2005; Otun et al., 2011). To our knowledge,

Table 3. MAP changes in nonpregnant rats after saline and LPS administration[a]

	Day 1	Day 2	Day 3	Day 4
Saline[b]	−0.35 (−0.75–0.18)	0.60 (−0.13–1.44)	2.07 (1.30–2.81)	−0.75 (−1.71–0.31)
LPS[b]	1.32 (−0.03–3.64)	3.68[c] (0.74–6.81)	0.21 (−1.29–1.89)	−1.04 (-3.46–1.31)

[a]Data were obtained from four non-pregnant animals receiving both saline and LPS injections; doses of saline and LPS were the same as the doses administered to pregnant rats.

[b]Data are represented as mean and (range) of MAP changes from baseline; baseline was calculated for each rat using the mean MAP recorded over the 2-d before the initiation of each treatment.

[c]$P < 0.01$ compared with the corresponding day of saline treatment.

our study provides the first evidence of an inhibitory role of TNF on interstitial trophoblast invasion in vivo. Few studies have quantitatively reported deficient interstitial trophoblast invasion in women with PE (Kadyrov et al., 2003; Naicker et al., 2003). However, the migration and invasion of interstitial trophoblast cells is an event that Vercruysse et al. (2006) described as being intimately associated with the maternal vascular network. It has been proposed that interstitial trophoblast cells play a role in the destruction of the tunica media of spiral arteries as part of the conditioning process required to accommodate endovascular trophoblast invasion and remodeling (Pijnenborg et al., 1983; Kam et al., 1999). Furthermore, intravasation of interstitial trophoblast cells into the spiral arteries is an important aspect of the vascular modification necessary for a healthy pregnancy (Kaufmann et al., 2003). Interestingly, our study also revealed that the extent of interstitial trophoblast invasion was positively correlated with cross-sectional area of spiral arteries.

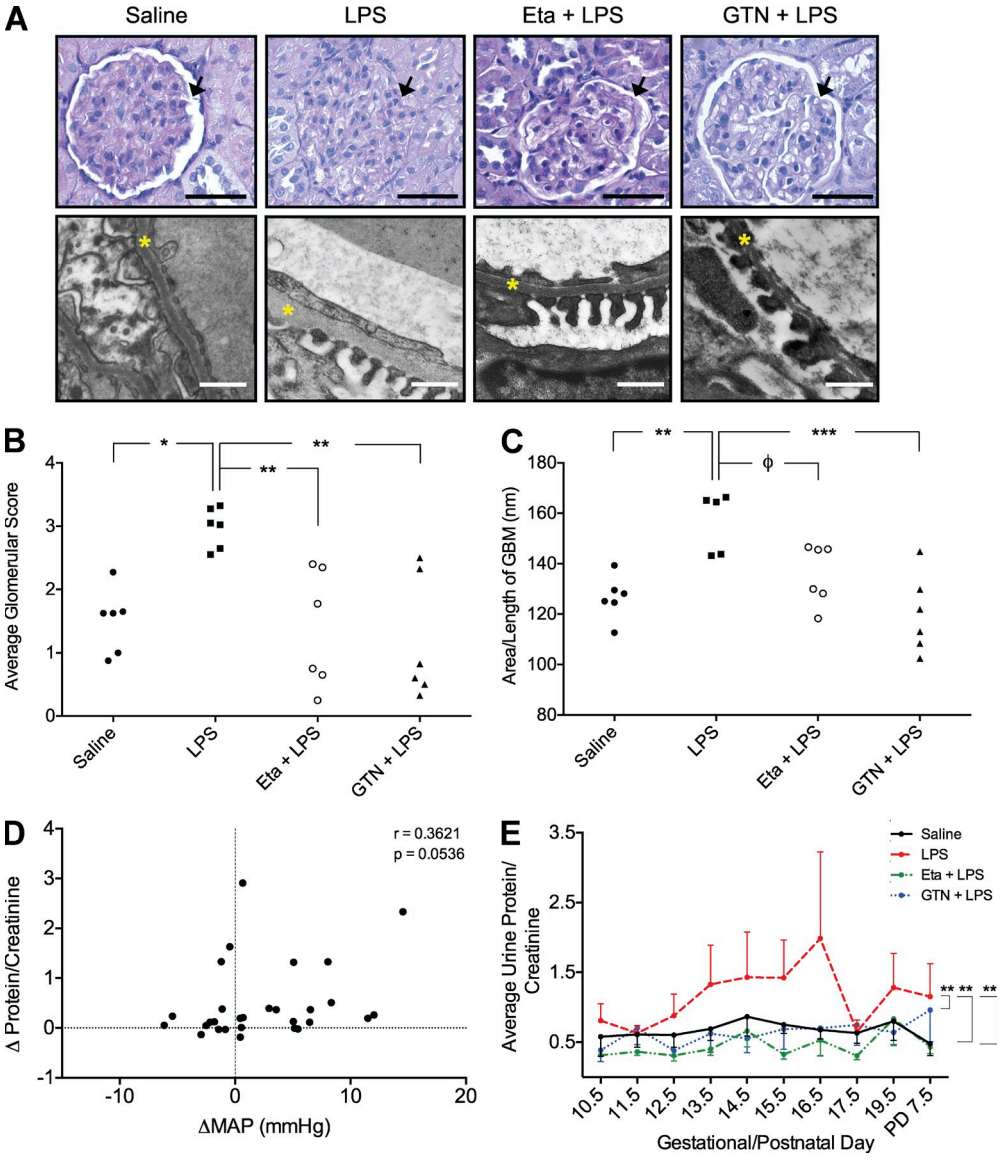

Figure 5. LPS-induced renal alterations and proteinuria are causally linked to TNF and can be prevented by GTN. Glomerular pathology of maternal kidneys from LPS-treated animals including hypercellularity, occlusion of the urinary space (arrows), and thickening of the GBM (yellow asterisks; A). Degree of glomerular pathology (mean of 20 glomeruli/animal; n = 5–6 animals/group; B) and assessment of GBM thickening across all treatment groups (C). Correlation between the change in MAP and change in urinary protein/creatinine from LPS-treated dams (D). Mean protein/creatinine ratio from urine collected on GD 10.5–16.5. 17.5, 19.5 and PD 7.5 across all treatment groups (E). The curves in E were generated using the mean ± SEM protein/creatinine ratios from urine collected from 3–5 rats/treatment group over the indicated GDs. Because of missing values and variability in the baseline protein/creatinine ratios before initiation of treatments, statistical analysis in (E) was performed on the changes in protein/creatinine ratios rather than on the actual raw values using ANOVA followed by Bonferroni post-hoc test. Φ, P = 0.0562; *, P < 0.05; **, P < 0.01. Bars: (top row) 50 µm; (bottom row) 500 nm.

In humans, early-onset PE, defined as arising before the 34th week of gestation, is often associated with the development of FGR (Valensise et al., 2008). Studies describing early-onset FGR/PE cite defective placentation and deficient SA remodeling as a leading cause of the inadequate uteroplacental perfusion and oxidative stress that characterize this pathology (Burton and Jauniaux, 2011). Here, we provide evidence that a deficiency in SA remodeling mediated by inflammation is associated with abnormal uteroplacental hemodynamics. Specifically, Doppler analysis revealed an increase in the RI of the spiral arteries from dams exposed to LPS compared with saline-treated controls. Moreover, we found that the effect of LPS on vascular resistance was mediated by TNF, given that Eta administration to LPS-treated animals normalized this parameter. Additionally, umbilical artery PSV was negatively correlated with SA RI only in LPS-treated animals. The premature reduction in umbilical artery PSV in fetuses from LPS-treated dams may be linked to placental dysfunction associated with poor fetal growth (Acharya et al., 2005). Furthermore, we observed a positive correlation between SA RI and maternal channel RI across all treatment groups. This finding indicates that alterations in perfusion may propagate downstream through vessels directly leading to the fetal-maternal interface. Clinically, umbilical and uterine artery velocimetry is used in screening for FGR and PE (van Asselt et al., 1998; Valensise et al., 2008; Byun et al., 2009). Fortunately, the unique vasculature of the rat uteroplacental network affords an opportunity to visualize and quantify SA flow in vivo using ultrasonography. This is an important feature lacking reliability and reproducibility in human cases (Collins et al., 2012).

In our study, FGR was clearly evident at GD 17.5 (4 d after the first LPS injection) and persisted at least until birth. However, by PD 7.5 the weights of pups from LPS-treated rats were not significantly different from the weights of pups from saline-treated rats. This finding is similar to what has been previously observed in humans, whereby children who are born growth restricted experience rapid catch-up growth during the first year of postnatal life (Boersma and Wit, 1997). Interestingly, by PD 7.5, pups from rats treated with Eta + LPS were significantly larger than pups from rats treated with either saline or LPS alone. The mechanism underlying this effect of Eta on postnatal growth requires further investigation.

While impaired fetal growth and development are the main consequences of placental insufficiency, the maternal response to altered perfusion may eventually manifest as PE. The two-stage hypothesis of PE proposes that placental oxidative/nitrosative stress causes the release of pro-inflammatory molecules central to the disease process (Borzychowski et al., 2006; Roberts and Gammill, 2005). Hypoxia/reoxygenation of chorionic villi explants increased TNF release and resulted in the activation maternal endothelial cells (Hung et al., 2004). Targeted inhibition of TNF in a model of myocardial ischemia reduced endothelial dysfunction and superoxide generation (Gao et al., 2008). Our study showed that abnormal placental perfusion mediated by excessive inflammation was associated with placental oxidative/nitrosative stress. This is a phenomenon also observed in human cases of early-onset PE associated with FGR (Yung et al., 2008). Interestingly, normalization of uteroplacental perfusion with the NO mimetic GTN (as revealed by Doppler ultrasonography) attenuated the accumulation of nitrotyrosine in the placenta and prevented FGR. Moreover, this normalization of uteroplacental perfusion in rats treated with GTN + LPS was closely associated with a dampened inflammatory response, as revealed by the much decreased circulating maternal TNF levels. Thus, we propose that the exaggerated inflammatory response that follows administration of low-dose LPS is a consequence of an inadequately perfused placenta. This concept is supported by the observation that LPS administration did not contribute to an exaggerated inflammatory response in nonpregnant rats.

Our data also indicate that the increases in MAP and the renal alterations observed in LPS-treated dams are a result of the inflammatory response triggered by LPS. Radiotelemetry experiments revealed that in saline-treated rats, MAP progressively decreased throughout gestation and remained low relative to baseline up to 7 d postpartum. Others have reported a similar MAP gestational profile in the rat (Dechend et al., 2005; Lau et al., 2013). Although the differences in MAP between LPS- and saline-treated rats were not very large, the magnitude observed was similar to that reported by others using instrumented pregnant Wistar rats injected with trophoblast cell debris (Lau et al., 2013).

In contrast to the blood pressure profile of women with PE, rats treated with LPS in our study did not exhibit a progressive increase in blood pressure toward the end of gestation after the initial acute rise in MAP. However, compared with the other treatment groups, MAP remained higher in LPS-treated rats until the postpartum period. For the majority of women with PE, hypertension resolves soon after birth; however, the timing of resolution is unclear and often debated. A recent study of >200 preeclamptic women revealed that at the time they were discharged from hospital, 78% were still hypertensive. Moreover, hypertension was found in 54% of women at 6 wk postpartum and in 39% of women by 3 mo postpartum (Berks et al., 2009).

The reduced uteroplacental perfusion (RUPP) model of PE is characterized by elevated blood pressure, and studies using this model revealed a physiological role for TNF as a key molecule mediating the elevation in blood pressure (LaMarca et al., 2005). In our study, administration of LPS resulted in a significant elevation in MAP that was mediated by TNF. High levels of TNF are known to play an inhibitory role in endothelium-dependent and NO-mediated vasodilation (Zhang et al., 2009). Moreover, there is evidence that TNF induces the release of the potent vasoconstrictor endothelin-1 (ET-1) from bovine aortic endothelial cells in a time- and concentration-dependent manner (Marsden and Brenner, 1992). Thus, we propose that Eta prevents the increase in MAP observed in LPS-treated pregnant rats, at least partly, by inhibiting TNF-mediated release of ET-1 by the maternal endothelium. Furthermore, our data revealed that transdermal administration of GTN attenuated the LPS-induced increase in MAP.

Studies indicate that the blood pressure lowering effects of NO donors are at least partly due to inhibition of ET-1–mediated vasoconstriction (Bourque et al., 2011; Bourque et al., 2012). Moreover, it has been reported that endothelium-derived NO inhibits the release of ET-1 from the porcine aorta (Boulanger and Lüscher, 1990) and that exogenous administration of NO inhibits *ET-1* gene transcription (Kourembanas et al., 1993). Therefore, it is likely that GTN prevents the increases in MAP observed in LPS-treated pregnant rats by interfering with a mechanism of vasoconstriction involving TNF-induced ET-1 activity. Through this mechanism GTN may also ensure adequate placental perfusion, thereby preventing the development of an exaggerated inflammatory response to LPS and the downstream sequelae. In addition to these indirect antiinflammatory actions of GTN, it is also possible that GTN has direct antiinflammatory properties. We have preliminary results indicating that GTN can inhibit in vitro TNF release by LPS-activated THP-1 cells, a monocytic cell line (unpublished data). Nevertheless, to our knowledge, the present study provides the first evidence that GTN can inhibit acute proinflammatory effects of LPS.

The critical role of the kidneys in the regulation and maintenance of blood pressure suggests that the maternal renal abnormalities, characteristic of PE, are closely linked to blood pressure alterations. Our rat model revealed that treatment with LPS resulted in renal alterations similar to those present in women with severe PE. These alterations included mesangial hypercellularity, occlusion of the capillary loops and urinary space, and thickening of the GBM. Renal abnormalities were not observed in dams treated with Eta + LPS or GTN + LPS. Our data agree with a recent study that mechanistically linked high levels of TNF and subsequent oxidative stress to hypertension and renal abnormalities in a mouse model of the chronic inflammatory autoimmune disorder systemic lupus erythematosus (Venegas-Pont et al., 2010).

Our conceptual model proposes that during pregnancy, an otherwise mild inflammatory stimulus causes severe restrictions in uteroplacental perfusion leading to FGR and an exaggerated maternal inflammatory response characterized by increased circulating TNF levels, increased MAP, and renal structural alterations. Whereas administration of LPS to nonpregnant rats led to a small increase in MAP, LPS administration to nonpregnant animals did not cause renal alterations and did not result in substantial increases in circulating WBCs and TNF levels.

Although we focused on investigating the role of abnormal inflammation in SA remodeling, we cannot rule out the possibility that other inflammation-related factors contribute to the pathogenesis of pregnancy complications. For example, abnormal inflammation may be linked to FGR/PE via disruption of hemostasis (Pijnenborg et al., 2006; Cotechini et al., 2012; Falcón et al., 2012), release of other proinflammatory molecules (Borzychowski et al., 2006), local placental damage (Burton et al., 2009), and/or syncytiotrophoblast microparticles (Knight et al., 1998) that may induce systemic endothelial dysfunction.

In addition to the nonpathological, low-grade inflammatory state of healthy pregnancy, normal pregnant women are more susceptible to infections compared with their nonpregnant counterparts (Mor and Cardenas, 2010). Indeed, our study and other studies found the effects of LPS to be pregnancy specific (Faas et al., 1994, 1995). Our study indicates that TNF levels in nonpregnant rats, measured 2 h after LPS administration, were not significantly different from TNF levels measured in saline-treated rats during pregnancy. The excessive inflammation characteristic of women afflicted by PE may therefore be an exacerbation of an underlying inflammatory pathology. Obesity, urinary tract infections, periodontal disease, and viral infections are associated with the development of PE (Conde-Agudelo et al., 2008; Rustveld et al., 2008; Chaparro et al., 2013). Based on our conceptual model, we propose that deficient placental perfusion is a critical aspect of the pathophysiology of FGR and PE associated with abnormal inflammation.

The use of LPS to trigger inflammation is well described and has been used to study the pathophysiology of various disease states including Parkinson's disease (Liu and Bing, 2011), acute lung injury (Rittirsch et al., 2008), and pathological pregnancies (Faas et al., 1994). Recently, Lin et al. (2012) reported that the endogenous antiinflammatory molecule Lipoxin A(4) could alleviate LPS-induced PE-like symptoms in pregnant Sprague–Dawley rats. The authors of that study did not report FGR, possibly because a single, lower dose of LPS was used. Although LPS is often used to induce sepsis, the doses used in our model were much lower than those required to induce septic shock in rodents (McDonald et al., 2000; Nemzek et al., 2008). In other studies, LPS has been used to induce preterm labor in mice (Salminen et al., 2008; Shynlova et al., 2013); however, with the low doses of LPS used in our study, we did not observe preterm labor.

Modulation of inflammation may have therapeutic benefit in the prevention and management of FGR/PE. Despite low transplacental transfer, Eta is currently classified as a category B drug by the United States Federal Drug Administration and is not routinely prescribed to pregnant women due to a lack of well-controlled prospective studies (Berthelsen et al., 2010). Two recent retrospective studies examining the safety of Eta use during pregnancy were conflicting. One study linked Eta to the development of congenital malformations (Carter et al., 2009), whereas the most recent report did not find increased incidence of malformations when compared with acceptable rates in Western countries (Viktil et al., 2012). The results of our study also highlight the potential use of NO-mimetics as antiinflammatory agents in the prevention of FGR/PE. The safety and use of GTN in obstetrics as a tocolytic agent are well characterized (Smith et al., 1999; de Pace et al., 2007).

In summary, our study demonstrates a novel mechanism by which abnormal maternal inflammation decreases SA remodeling associated with deficient uteroplacental perfusion and the development of FGR/PE. Given the similarities of hemochorial placentation between humans and rats, in particular

the pattern of deep intrauterine trophoblast invasion and SA remodeling (Soares et al., 2012), we believe that our rat model of LPS-induced FGR/PE is useful for the study of inflammation-associated pregnancy complications. The results of our study indicate that judicious management of inflammation, either systemically or by blocking the release of placental proinflammatory molecules, is a potential strategy for the prevention and/or treatment of FGR/PE.

MATERIALS AND METHODS

Animals. Studies were conducted in accordance with the guidelines of the Canadian Council on Animal Care and protocols were approved by the Queen's University Animal Care Committee. Virgin female Wistar rats (3–6 mo old; Charles River Laboratories) were housed in a light- and humidity-controlled environment and fed ad libitum with free access to tap water. Vaginal smears were performed the morning after females were housed overnight with a fertile male at a 2:1 ratio. The presence of spermatozoa in the vaginal lavage confirmed pregnancy and was designated GD 0.5.

Experimental protocol. Pregnant rats received i.p. injections of saline or LPS (*Escherichia coli* serotype 0111:B4; Sigma-Aldrich) on GD 13.5, 14.5, 15.5, and 16.5 of a 22-d gestation. To induce an inflammatory response, dams received a single low dose (10 µg/kg) of LPS on GD 13.5, followed by higher doses (40 µg/kg) daily until GD 16.5 (n = 28). Control animals (n = 22) received saline (1 ml/kg) injections on the corresponding GDs. Rats received 5 ml of lactated ringers subcutaneously with each injection. Dams were sacrificed 24 h after the last LPS/saline injection on GD 17.5. Animals used in the radiotelemetry experiments (see below) were sacrificed on PD 7.5. After euthanasia, fetal weights were measured and recorded in conjunction with the pup's location along the length of the uterine horn. To evaluate the role of TNF on the development of FGR, dams additionally received i.p. injections of the TNF inhibitor Eta (10 mg/kg; Enbrel; Amgen and Wyeth Pharmaceuticals) on GD 13.5 and 15.5, 6 h before administration of LPS (n = 16). To determine whether the effects of LPS are pregnancy specific, nonpregnant rats were exposed to the same doses of LPS as pregnant animals over 4 d (10 µg/kg followed by 40 µg/kg) and sacrificed on the fifth day, 24 h after the last LPS injection. To examine the acute effects of LPS, additional experiments were performed on rats 2 h after the initial LPS (10 µg/kg) injection. For these studies, maternal blood was collected at euthanasia from rats across all treatment groups on GD 13.5, 2 h after LPS administration (n = 5–7). Corresponding experiments were performed on nonpregnant rats 2 h after saline or LPS administration (n = 4).

Administration of GTN. To assess a potential role of deficient NO signaling in the pathogenesis of inflammation-induced FGR/PE, pregnant dams (n = 16) receiving LPS were additionally treated with the NO-mimetic GTN. This was accomplished via daily application and replacement of Minitran transdermal patches (Graceway Pharmaceuticals) starting on GD 12.5 and ending on GD 16.5. Patches (cut to a surface area of 1.7 cm^2, providing a GTN steady-state delivery rate of 25 µg/h) were placed on the nape of the neck and were covered with a thin layer of New Skin Liquid Bandage (Prestige Brands Inc.). The last patch was removed at euthanasia on GD 17.5.

Tissue preparation. Rats were sacrificed on GD 17.5 via an i.p. injection (40–50 mg/kg) of sodium pentobarbital (Ceva Santé Animale). Following euthanasia, the wet weight of each fetus was measured and recorded in combination with its location along the length of the respective uterine horn. Implantation sites (uterus + placenta) were placed in 4% paraformaldehyde for at least 24 h. Before tissue processing, implantation sites were carefully bisected (through the MT and placenta) to ensure that the mid-portion of each unit was used for further analysis. Tissues were subsequently transferred to 70% ethanol and were processed and embedded in paraffin according to standard procedures. Serial sections (5 µm) were cut from each uteroplacental unit for immunohistochemical analysis.

Identification of trophoblast and smooth muscle cells. Trophoblast cells were identified by immunohistochemistry for cytokeratin using mouse monoclonal anticytokeratin antibody (DAKO) and the method described by Vercruysse et al. (2006). Negative controls consisted of sections in which the primary antibody was substituted with an equal concentration of mouse IgG (DAKO).

Immunohistochemistry for α-actin was used to identify vascular smooth muscle cells. In brief, tissues were rehydrated using a graded ethanol series and sections were subsequently blocked using 10% normal horse serum (NHS) + 0.1% Tween-80 (Thermo Fisher Scientific) for 20 min followed by serum-free DAKO block for 7 min. Sections were then incubated for 30 min in the presence of antibody against smooth muscle α-actin (Sigma-Aldrich; 1:400 in 2% NHS); this was followed by incubation with biotinylated anti–mouse IgG antibody (1:200 in 1% NHS + 3% normal rat serum; 30 min; Vector Laboratories). A Vectastain ABC Elite kit (Vector Laboratories) and diaminobenzidine (DAKO) were used to detect antigenic sites. Tissues were counterstained with Gill's hematoxylin (Thermo Fisher Scientific), dehydrated, and mounted. Negative controls consisted of sections incubated with an equal concentration of mouse IgG (DAKO) in place of the primary α-actin antibody.

Identification of tissue macrophages using CD68 immunohistochemistry. After rehydration, proteinase K antigen retrieval in sections of implantation sites was performed, and endogenous peroxidase was quenched using 3% H_2O_2 + 0.3% Triton X-100 (Bio-Rad Laboratories) in PBS. Nonspecific sites in sections were subsequently blocked using 10% NHS for 20 min, followed by serum-free DAKO block for 7 min (DAKO). Primary antibody (AbD Serotec; 1:250 in 2% NHS) was added overnight at 4°C. Secondary antibody (1:200 in 1% NHS; Vector Laboratories) was added for 30 min and detected using the Vectastain ABC Elite kit (Vector Laboratories). Sections were developed using diaminobenzidine (DAKO), counterstained with Gill's hematoxylin (Thermo Fisher Scientific), dehydrated, and mounted. Negative controls consisted of sections in which primary antibody was substituted with equal concentrations of mouse IgG (DAKO).

Image analysis. Assessment of activated macrophage localization, interstitial trophoblast invasion, and SA remodeling was performed on slides scanned at 20× using an Aperio ImageScope system and software (Aperio). A positive pixel count was used to quantify labeled cells in the MT to assess the presence of activated macrophages. Interstitial trophoblast invasion was calculated as the total area occupied by cytokeratin-positive interstitial trophoblast cells within the MT. Only sections exhibiting the "break through" of interstitial trophoblast cells through the giant cell layer were used to quantify interstitial invasion for consistency (Bridgman, 1948). The cross-sectional area of spiral arteries exhibiting endovascular trophoblast cells was measured by a blinded observer and confirmed by a second investigator. Specifically, the fibrinoid layer around spiral arteries and/or the basal surface of cytokeratin-positive or endothelial cells were used as the boundary with which to manually delineate the luminal contour of each vessel.

Doppler ultrasonography. Doppler ultrasonography was used to evaluate maternal and fetal hemodynamic alterations on GD 17.5 using a previously described method (Renaud et al., 2011) adapted from Mu and Adamson (2006). In brief, abdominal hair was removed from anaesthetized (~3% isoflurane in oxygen by nose cone) dams using a mechanical shaver followed, by application of a chemical depilatory. Maternal heart rate and breathing were monitored constantly to ensure surgical plane for the duration of the measurements. The high frame rate 707B 30 mHz scanhead was used in Doppler mode to obtain pulse-wave recordings for offline analysis. Data acquisition was performed on 3–4 viable implantation sites per dam; measurements were recorded from an implantation site located adjacent to the bladder and a site in close proximity to the ovary within each horn. Doppler waveforms were recorded for 2–3 spiral arteries and the corresponding fetal umbilical artery for each implantation site. After acquisition, a blinded observer performed analysis. PSV and end diastolic flow velocity (EDV) of each SA was measured to determine the mean SA RI of the implantation site based on the following

equation (RI = [PSV – EDV]/PSV). Umbilical PSV of the corresponding implantation site was also measured.

Complete blood cell counts (CBCs). Whole blood was collected by cardiac puncture into tubes containing ethylenediaminetetraacetic acid (EDTA) for CBC analysis. Blood samples (12 µl) were analyzed using the ABC Vet Animal Blood Counter (Scil Animal Care Company) according to the manufacturer's instructions.

Analysis of maternal plasma TNF. To confirm that LPS administration induced maternal inflammation, plasma levels of TNF were quantified by ELISA (R&D Systems) according to the manufacturer's instructions. Levels falling below the minimum detectable dose of the kit (5 pg/ml) were considered undetectable. At euthanasia, maternal blood was collected via cardiac puncture into EDTA-containing syringes to prevent clotting. Blood samples were obtained from dams at the following time-points: 2 h after saline or LPS ± Eta/GTN administration at GD 13.5; 2 h after LPS administration at GD 15.5; 2 h after LPS administration to nonpregnant animals.

Implantation of radiotelemetry transducers. Continuous assessment of MAP was achieved through femoral implantation of PA-C40 radiotransmitters (Data Sciences International). In brief, virgin female rats were anaesthetized using ∼3.0% isoflurane in oxygen by nose cone. The left thigh was shaved, and a 2-cm incision was made to expose the femoral vessels and nerve. Using a dissection microscope, the femoral artery was carefully retracted, and a permanent occlusion suture was placed around the vessel. Proximal to the occlusion ligature, a 26-gauge needle was used to puncture the vessel to facilitate the insertion of the tip of the transmitter catheter. Cannulation forceps were used to advance the catheter tip into the abdominal aorta, whereupon sutures were used to hold the device in place. Transmitters were secured subcutaneously over the right flank and the incision was closed with staples. Postoperative care consisted of administration of meloxicam (1 mg/kg), dexamethasone (0.05 mg/kg), and tramadol (20 mg/kg) in 10 ml of subcutaneous lactated ringers administered daily for 4–7 d as needed. Dams were allowed to recover for at least 14 d before overnight mating. Pregnant animals were randomized into the four treatment groups (n = 5/group): saline, LPS, Eta + LPS, and GTN + LPS. Dams and pups were euthanized on PD 7.5.

Radiotelemetry data acquisition and representation. Upon recovery, continuous 24-h data were collected for 30 s every 8 min using Dataquest A.R.T. Acquisition System (Data Sciences International, version 4.1) until the study endpoint at PD 7.5. All values from a 24-h period (midnight–midnight) were used to calculate a daily 24-h mean data point for each GD. Although absolute MAP values exhibited a normal range of variability among groups before treatments started, importantly, MAP profiles did not differ significantly between animals before treatment initiation (GD 0–11). To evaluate the effect of treatment on changes in blood pressure, MAP measured on GD 11 was set as baseline for each animal, and the delta value was calculated for subsequent GDs/PDs. To determine whether the effects of LPS on MAP are pregnancy-specific, we performed an additional set of experiments on nonpregnant animals. Animals in the nonpregnant study group (n = 4) were instrumented with radiotelemetry transducers, as previously described. After recovery, all animals were subjected to the following procedures: 2 d of baseline recording; four saline injections (once/day); 1 d of rest; 2 d of baseline recording; four LPS injections (10–40 µg/kg/day, as per the doses used in the pregnancy studies). For each experimental animal, MAP recorded over the 2 d preceding the onset of each treatment was set as baseline, and the delta value was determined for subsequent experimental days. Baseline MAP before the onset of saline treatment was not significantly different than baseline MAP before LPS administration.

Urine analysis. Urine was collected from animals instrumented with radiotransmitters on GD 10.5–17.5, GD 19.5, and PD 7.5 using a modified metabolic cage technique. For all days of urine collection that corresponded with injection days, urine was collected in the morning, before animals received any treatment. In brief, dams were placed in cages lined with 96-well plates for 3–4 h on the morning of collection. Urine was collected from the plates and centrifuged (300 g, for 5 min) before storing at −80°C for future analysis. Total protein concentration was determined using a protein assay (Bio-Rad Laboratories) and was normalized against total creatinine concentration (Cayman Chemical Company) to assess proteinuria. Because each animal had different protein/creatinine ratios before the onset of any treatment, a baseline protein/creatinine measurement for each rat was determined by taking the mean protein/creatinine values from urine collected each day from GD 10.5 to 12.5. This baseline protein/creatinine ratio was used to calculate the change in proteinuria from urine collected on subsequent days after initiation of treatments. To determine whether proteinuria correlates with changes in MAP, changes in protein/creatinine ratios were matched against corresponding changes in MAP for all animals in each treatment group.

Assessment of postnatal pup weight. Pups from all treatment groups were weighed on PD 1.5 and 7.5. It has recently been suggested that the standardization of litter sizes is beneficial to account for litter size–induced effects (i.e., physical space restraints and access to maternal milk supplies), which would otherwise dilute the ability to detect treatment-related outcomes on fetal growth and postnatal development. Given that pup weight assessment was performed several days after treatment was administered and may have affected litter sizes, we applied a correction factor to standardize pup weights based on litter size as described by Chahoud and Paumgartten (2009).

Histopathological analysis of kidneys. Kidneys harvested from dams on GD 17.5 were fixed, processed, sectioned (3 µm), and stained with hematoxylin and eosin and periodic acid-Schiff for histopathological assessment of renal alterations. The degree of glomerular pathology was assessed by a blinded observer based on criteria and scoring methods adapted from other studies (Strevens et al., 2003; Li et al., 2007), and after consultation with an experienced renal pathologist at Kingston General Hospital. For each kidney, 20 glomeruli were individually scored and the severity of glomerular pathology was determined from the mean score for each kidney. Confirmatory scoring was performed on each section by an additional blinded observer to ensure that mean scores for each section were consistent. Glomeruli from nonpregnant animals exposed to the same doses of LPS (n = 4) were additionally assessed as previously described.

Electron microscopic analysis of renal ultrastructure. Glutaraldehyde-fixed 1-mm^3 cortical samples from kidneys were processed, embedded in epon, and cut into ultra-thin (90-nm) sections. Images captured by a blinded observer were later used to evaluate ultrastructural alterations of the GBM. Quantitative assessment of GBM thickness (GBM area/GBM length) was performed using Image-Pro Plus version 6.0 software.

Quantitative analysis of placental nitrotyrosine. Placental nitrotyrosine levels were quantified by ELISA using a commercially available kit (Millipore). As previously described (Roberts et al., 2009), placentas randomly chosen from all treatment groups were homogenized in lysis buffer on ice using a Polytron tissue homogenizer (Biospec Products Inc.). Homogenates were centrifuged (20,000 g, for 5 min) and the supernatant was transferred to separate tubes. A modified Lowry assay (DC Protein Assay; Bio-Rad Laboratories) was used to measure and subsequently adjust protein concentrations between samples. Samples (saline, n = 9 from seven mothers; LPS, n = 21 from nine mothers; LPS + GTN, n = 9 from seven mothers) were assayed in duplicate.

Statistics. Data were analyzed using GraphPad Prism 6.0 Software (GraphPad). Parametric data are presented as mean ± SEM and were analyzed using two-tailed Student's t test (two groups), one-way ANOVA (three or more groups), or two-way ANOVA (two-variables). Significant differences between individual treatment groups were determined using the Bonferroni post-hoc test when comparing fewer than five groups, or Tukey's multiple comparison post-hoc test when comparing more than five groups. Kruskal-Wallis followed by Dunn's multiple comparison post-hoc test was used to

assess alterations in maternal plasma TNF levels, as these did not follow a normal distribution. χ^2 was used to analyze data obtained from nitrotyrosine determination experiments. For the radiotelemetry studies in pregnant animals, changes in MAP relative to baseline (GD 11) were analyzed using repeated measures two-way ANOVA, followed by Bonferroni post-hoc test to assess for statistical differences between groups. Within each treatment group, differences in raw MAP from baseline (GD 11) were determined by repeated measures two-way ANOVA, followed by Dunnett's multiple comparisons test. Expectation maximization imputation was performed for data points missing at random (a total of six data points) from the radiotelemetry experiments using SPSS Statistics software. This method has been previously used and validated for imputation of missing data in rat studies using small sample sizes (Rubin et al., 2007). Changes in MAP relative to baseline in nonpregnant animals were analyzed using repeated measures two-way ANOVA, followed by Bonferroni post-hoc test to assess for statistical differences between groups. To compare overall differences in proteinuria, the mean change of the protein/creatinine ratio was calculated for each day of urine collection and analyzed using one-way ANOVA, followed by Bonferroni post-hoc test. Nonlinear, nonparametric data were assessed by Spearman correlation, whereas linear parametric data were assessed by Pearson correlation. For all statistical tests, $P < 0.05$ was considered significant, whereas $P < 0.1$ was considered a trend toward significance.

We would like to thank the following individuals: Professor Robert Pijnenborg and Lisbeth Vercruysse for sharing their technical knowledge of cytokeratin and α-actin staining; Kim Laverty for performing radiotelemetry surgeries; John DaCosta, Oliver Jones, and Xiahou Yan for tissue processing for light and electron microscopy; Shakeel Virk for scanning slides and providing access to the Aperio Digital microscope; Dr. Iain Young for assistance with the histopathological assessment of glomeruli; Kevin Robb and Chelsea Smallwood for performing blinded ultrasound and histological analysis; Kristiina Aasa and Jalna Meens for assistance with ultrasound image acquisition; Wilma Hopman for assistance with statistics; Deborah Harrington for technical assistance with CBC data collection; and Dr. Chandrakant Tayade for comments and suggestions during the preparation of the manuscript.

This work was supported by a grant from the Canadian Institutes of Health Research (CIHR) awarded to C.H. Graham. T. Cotechini is the recipient of a CIHR Doctoral Award-Frederick Banting and Charles Best Canada Graduate Scholarship and an Ontario Graduate Scholarship.

The authors have no conflicting financial assistance.

Submitted: 8 February 2013
Accepted: 20 November 2013

REFERENCES

Acharya, G., T. Wilsgaard, G.K. Berntsen, J.M. Maltau, and T. Kiserud. 2005. Reference ranges for serial measurements of blood velocity and pulsatility index at the intra-abdominal portion, and fetal and placental ends of the umbilical artery. *Ultrasound Obstet. Gynecol.* 26:162–169. http://dx.doi.org/10.1002/uog.1902

Bauer, S., J. Pollheimer, J. Hartmann, P. Husslein, J.D. Aplin, and M. Knöfler. 2004. Tumor necrosis factor-alpha inhibits trophoblast migration through elevation of plasminogen activator inhibitor-1 in first-trimester villous explant cultures. *J. Clin. Endocrinol. Metab.* 89:812–822. http://dx.doi.org/10.1210/jc.2003-031351

Berks, D., E.A. Steegers, M. Molas, and W. Visser. 2009. Resolution of hypertension and proteinuria after preeclampsia. *Obstet. Gynecol.* 114: 1307–1314.

Berthelsen, B.G., H. Fjeldsøe-Nielsen, C.T. Nielsen, and E. Hellmuth. 2010. Etanercept concentrations in maternal serum, umbilical cord serum, breast milk and child serum during breastfeeding. *Rheumatology (Oxford).* 49:2225–2227. http://dx.doi.org/10.1093/rheumatology/keq185

Boersma, B., and J.M. Wit. 1997. Catch-up growth. *Endocr. Rev.* 18:646–661. http://dx.doi.org/10.1210/er.18.5.646

Borzychowski, A.M., I.L. Sargent, and C.W. Redman. 2006. Inflammation and pre-eclampsia. *Semin. Fetal Neonatal Med.* 11:309–316. http://dx.doi.org/10.1016/j.siny.2006.04.001

Boulanger, C., and T.F. Lüscher. 1990. Release of endothelin from the porcine aorta. Inhibition by endothelium-derived nitric oxide. *J. Clin. Invest.* 85:587–590. http://dx.doi.org/10.1172/JCI114477

Bourque, S.L., S.T. Davidge, and M.A. Adams. 2011. The interaction between endothelin-1 and nitric oxide in the vasculature: new perspectives. *Am. J. Physiol. Regul. Integr. Comp. Physiol.* 300:R1288–R1295. http://dx.doi.org/10.1152/ajpregu.00397.2010

Bourque, S.L., H.A. Whittingham, S.E. Brien, S.T. Davidge, and M.A. Adams. 2012. Role of endothelin-1 in the hyper-responsiveness to nitrovasodilators following acute NOS inhibition. *Br. J. Pharmacol.* 165:1992–1999. http://dx.doi.org/10.1111/j.1476-5381.2011.01696.x

Boyd, J.D., and W.J. Hamilton. 1970. The Human Placenta. W. Heffer and Sons Ltd., Cambridge, England. 137 pp.

Bridgman, J. 1948. A morphological study of the development of the placenta of the rat; an histological and cytological study of the development of the chorioallantoic palcenta of the white rat. *J. Morphol.* 83:195–223. http://dx.doi.org/10.1002/jmor.1050830204

Burton, G.J., and E. Jauniaux. 2011. Oxidative stress. *Best Pract. Res. Clin. Obstet. Gynaecol.* 25:287–299. http://dx.doi.org/10.1016/j.bpobgyn.2010.10.016

Burton, G.J., A.W. Woods, E. Jauniaux, and J.C. Kingdom. 2009. Rheological and physiological consequences of conversion of the maternal spiral arteries for uteroplacental blood flow during human pregnancy. *Placenta.* 30:473–482. http://dx.doi.org/10.1016/j.placenta.2009.02.009

Byun, Y.J., H.S. Kim, J.I. Yang, J.H. Kim, H.Y. Kim, and S.J. Chang. 2009. Umbilical artery Doppler study as a predictive marker of perinatal outcome in preterm small for gestational age infants. *Yonsei Med. J.* 50:39–44. http://dx.doi.org/10.3349/ymj.2009.50.1.39

Carter, J.D., A. Ladhani, L.R. Ricca, J. Valeriano, and F.B. Vasey. 2009. A safety assessment of tumor necrosis factor antagonists during pregnancy: a review of the Food and Drug Administration database. *J. Rheumatol.* 36:635–641. http://dx.doi.org/10.3899/jrheum.080545

Chahoud, I., and F.J. Paumgartten. 2009. Influence of litter size on the postnatal growth of rat pups: is there a rationale for litter-size standardization in toxicity studies? *Environ. Res.* 109:1021–1027. http://dx.doi.org/10.1016/j.envres.2009.07.015

Chaparro, A., A. Sanz, A. Quintero, C. Inostroza, V. Ramirez, F. Carrion, F. Figueroa, R. Serra, and S.E. Illanes. 2013. Increased inflammatory biomarkers in early pregnancy is associated with the development of preeclampsia in patients with periodontitis: a case control study. *J. Periodontal Res.* 48:302–307. http://dx.doi.org/10.1111/jre.12008

Collins, S.L., J.S. Birks, G.N. Stevenson, A.T. Papageorghiou, J.A. Noble, and L. Impey. 2012. Measurement of spiral artery jets: general principles and differences observed in small-for-gestational-age pregnancies. *Ultrasound Obstet. Gynecol.* 40:171–178. http://dx.doi.org/10.1002/uog.10149

Conde-Agudelo, A., J. Villar, and M. Lindheimer. 2008. Maternal infection and risk of preeclampsia: systematic review and metaanalysis. *Am. J. Obstet. Gynecol.* 198:7–22. http://dx.doi.org/10.1016/j.ajog.2007.07.040

Conrad, K.P., T.M. Miles, and D.F. Benyo. 1998. Circulating levels of immunoreactive cytokines in women with preeclampsia. *Am. J. Reprod. Immunol.* 40:102–111. http://dx.doi.org/10.1111/j.1600-0897.1998.tb00398.x

Cotechini, T., M. Othman, and C.H. Graham. 2012. Nitroglycerin prevents coagulopathies and foetal death associated with abnormal maternal inflammation in rats. *Thromb. Haemost.* 107:864–874. http://dx.doi.org/10.1160/TH11-10-0730

de Pace, V., G. Chiossi, and F. Facchinetti. 2007. Clinical use of nitric oxide donors and L-arginine in obstetrics. *J. Matern. Fetal Neonatal Med.* 20:569–579. http://dx.doi.org/10.1080/14767050701419458

Dechend, R., P. Gratze, G. Wallukat, E. Shagdarsuren, R. Plehm, J.H. Bräsen, A. Fiebeler, W. Schneider, S. Caluwaerts, L. Vercruysse, et al. 2005. Agonistic autoantibodies to the AT1 receptor in a transgenic rat model of preeclampsia. *Hypertension.* 45:742–746. http://dx.doi.org/10.1161/01.HYP.0000154785.50570.63

Faas, M.M., G.A. Schuiling, J.F. Baller, C.A. Visscher, and W.W. Bakker. 1994. A new animal model for human preeclampsia: ultra-low-dose endotoxin infusion in pregnant rats. *Am. J. Obstet. Gynecol.* 171:158–164. http://dx.doi.org/10.1016/0002-9378(94)90463-4

Faas, M.M., G.A. Schuiling, J.F. Baller, and W.W. Bakker. 1995. Glomerular inflammation in pregnant rats after infusion of low dose endotoxin.

An immunohistological study in experimental pre-eclampsia. *Am. J. Pathol.* 147:1510–1518.

Faas, M.M., M. Broekema, H. Moes, G. van der Schaaf, M.J. Heineman, and P. de Vos. 2004. Altered monocyte function in experimental preeclampsia in the rat. *Am. J. Obstet. Gynecol.* 191:1192–1198. http://dx.doi.org/10.1016/j.ajog.2004.03.041

Falcón, B.J., T. Cotechini, S.K. Macdonald-Goodfellow, M. Othman, and C.H. Graham. 2012. Abnormal inflammation leads to maternal coagulopathies associated with placental haemostatic alterations in a rat model of foetal loss. *Thromb. Haemost.* 107:438–447. http://dx.doi.org/10.1160/TH11-09-0626

Gao, X., H. Zhang, S. Belmadani, J. Wu, X. Xu, H. Elford, B.J. Potter, and C. Zhang. 2008. Role of TNF-alpha-induced reactive oxygen species in endothelial dysfunction during reperfusion injury. *Am. J. Physiol. Heart Circ. Physiol.* 295:H2242–H2249. http://dx.doi.org/10.1152/ajpheart.00587.2008

Gardosi, J., A. Chang, B. Kalyan, D. Sahota, and E.M. Symonds. 1992. Customised antenatal growth charts. *Lancet.* 339:283–287. http://dx.doi.org/10.1016/0140-6736(92)91342-6

Germain, S.J., G.P. Sacks, S.R. Sooranna, I.L. Sargent, and C.W. Redman. 2007. Systemic inflammatory priming in normal pregnancy and preeclampsia: the role of circulating syncytiotrophoblast microparticles. *J. Immunol.* 178: 5949–5956.

Hamai, Y., T. Fujii, T. Yamashita, H. Nishina, S. Kozuma, Y. Mikami, and Y. Taketani. 1997. Evidence for an elevation in serum interleukin-2 and tumor necrosis factor-alpha levels before the clinical manifestations of preeclampsia. *Am. J. Reprod. Immunol.* 38:89–93. http://dx.doi.org/10.1111/j.1600-0897.1997.tb00281.x

Hung, T.H., D.S. Charnock-Jones, J.N. Skepper, and G.J. Burton. 2004. Secretion of tumor necrosis factor-alpha from human placental tissues induced by hypoxia-reoxygenation causes endothelial cell activation in vitro: a potential mediator of the inflammatory response in preeclampsia. *Am. J. Pathol.* 164:1049–1061. http://dx.doi.org/10.1016/S0002-9440(10)63192-6

Hunt, J.S. 1989. Macrophages in human uteroplacental tissues: a review. *Am. J. Reprod. Immunol.* 21:119–122. http://dx.doi.org/10.1111/j.1600-0897.1989.tb01015.x

Jain, K., V. Kavi, C.V. Raghuveer, and R. Sinha. 2007. Placental pathology in pregnancy-induced hypertension (PIH) with or without intrauterine growth retardation. *Indian J. Pathol. Microbiol.* 50:533–537.

Kadyrov, M., C. Schmitz, S. Black, P. Kaufmann, and B. Huppertz. 2003. Pre-eclampsia and maternal anaemia display reduced apoptosis and opposite invasive phenotypes of extravillous trophoblast. *Placenta.* 24:540–548. http://dx.doi.org/10.1053/plac.2002.0946

Kam, E.P., L. Gardner, Y.W. Loke, and A. King. 1999. The role of trophoblast in the physiological change in decidual spiral arteries. *Hum. Reprod.* 14:2131–2138. http://dx.doi.org/10.1093/humrep/14.8.2131

Kaufmann, P., S. Black, and B. Huppertz. 2003. Endovascular trophoblast invasion: implications for the pathogenesis of intrauterine growth retardation and preeclampsia. *Biol. Reprod.* 69:1–7. http://dx.doi.org/10.1095/biolreprod.102.014977

Knight, M., C.W.G. Redman, E.A. Linton, and I.L. Sargent. 1998. Shedding of syncytiotrophoblast microvilli into the maternal circulation in pre-eclamptic pregnancies. *Br. J. Obstet. Gynaecol.* 105:632–640. http://dx.doi.org/10.1111/j.1471-0528.1998.tb10178.x

Knöfler, M., M. Stenzel, and P. Husslein. 1998. Shedding of tumour necrosis factor receptors from purified villous term trophoblasts and cytotrophoblastic BeWo cells. *Hum. Reprod.* 13:2308–2316. http://dx.doi.org/10.1093/humrep/13.8.2308

Koga, K., Y. Osuga, T. Tajima, Y. Hirota, T. Igarashi, T. Fujii, T. Yano, and Y. Taketani. 2010. Elevated serum soluble fms-like tyrosine kinase 1 (sFlt1) level in women with hydatidiform mole. *Fertil. Steril.* 94:305–308. http://dx.doi.org/10.1016/j.fertnstert.2009.02.015

Kourembanas, S., L.P. McQuillan, G.K. Leung, and D.V. Faller. 1993. Nitric oxide regulates the expression of vasoconstrictors and growth factors by vascular endothelium under both normoxia and hypoxia. *J. Clin. Invest.* 92:99–104. http://dx.doi.org/10.1172/JCI116604

LaMarca, B.B., W.A. Bennett, B.T. Alexander, K. Cockrell, and J.P. Granger. 2005. Hypertension produced by reductions in uterine perfusion in the pregnant rat: role of tumor necrosis factor-alpha. *Hypertension.* 46:1022–1025. http://dx.doi.org/10.1161/01.HYP.0000175476.26719.36

LaMarca, B.D., M.J. Ryan, J.S. Gilbert, S.R. Murphy, and J.P. Granger. 2007. Inflammatory cytokines in the pathophysiology of hypertension during preeclampsia. *Curr. Hypertens. Rep.* 9:480–485. http://dx.doi.org/10.1007/s11906-007-0088-1

Lau, S.Y., C.J. Barrett, S.J. Guild, and L.W. Chamley. 2013. Necrotic trophoblast debris increases blood pressure during pregnancy. *J. Reprod. Immunol.* 97:175–182. http://dx.doi.org/10.1016/j.jri.2012.12.005

Li, Z., Y. Zhang, J. Ying Ma, A.M. Kapoun, Q. Shao, I. Kerr, A. Lam, G. O'Young, F. Sannajust, P. Stathis, et al. 2007. Recombinant vascular endothelial growth factor 121 attenuates hypertension and improves kidney damage in a rat model of preeclampsia. *Hypertension.* 50:686–692. http://dx.doi.org/10.1161/HYPERTENSIONAHA.107.092098

Lin, F., P. Zeng, Z. Xu, D. Ye, X. Yu, N. Wang, J. Tang, Y. Zhou, and Y. Huang. 2012. Treatment of Lipoxin A(4) and its analogue on low-dose endotoxin induced preeclampsia in rat and possible mechanisms. *Reprod. Toxicol.* 34:677–685. http://dx.doi.org/10.1016/j.reprotox.2012.09.009

Liu, M., and G. Bing. 2011. Lipopolysaccharide animal models for Parkinson's disease. *Parkinsons Dis.* 2011:327089.

Lowe, D.T. 2000. Nitric oxide dysfunction in the pathophysiology of preeclampsia. *Nitric Oxide.* 4:441–458. http://dx.doi.org/10.1006/niox.2000.0296

Lyall, F., and M. Belfort. 2007. Pre-eclampsia: Etiology and Clinical Practice. Cambridge University Press, Cambridge.

Marsden, P.A., and B.M. Brenner. 1992. Transcriptional regulation of the endothelin-1 gene by TNF-alpha. *Am. J. Physiol.* 262:C854–C861.

McDonald, T.E., M.N. Grinman, C.M. Carthy, and K.R. Walley. 2000. Endotoxin infusion in rats induces apoptotic and survival pathways in hearts. *Am. J. Physiol. Heart Circ. Physiol.* 279:H2053–H2061.

Mor, G., and I. Cardenas. 2010. The immune system in pregnancy: a unique complexity. *Am. J. Reprod. Immunol.* 63:425–433. http://dx.doi.org/10.1111/j.1600-0897.2010.00836.x

Mu, J., and S.L. Adamson. 2006. Developmental changes in hemodynamics of uterine artery, utero- and umbilicoplacental, and vitelline circulations in mouse throughout gestation. *Am. J. Physiol. Heart Circ. Physiol.* 291:H1421–H1428. http://dx.doi.org/10.1152/ajpheart.00031.2006

Naicker, T., S.M. Khedun, J. Moodley, and R. Pijnenborg. 2003. Quantitative analysis of trophoblast invasion in preeclampsia. *Acta Obstet. Gynecol. Scand.* 82:722–729. http://dx.doi.org/10.1034/j.1600-0412.2003.00220.x

Nemzek, J.A., K.M. Hugunin, and M.R. Opp. 2008. Modeling sepsis in the laboratory: merging sound science with animal well-being. *Comp. Med.* 58:120–128.

Otun, H.A., G.E. Lash, B.A. Innes, J.N. Bulmer, K. Naruse, T. Hannon, R.F. Searle, and S.C. Robson. 2011. Effect of tumour necrosis factor-α in combination with interferon-γ on first trimester extravillous trophoblast invasion. *J. Reprod. Immunol.* 88:1–11. http://dx.doi.org/10.1016/j.jri.2010.10.003

Page, E. 1939. The relation between hydatid moles, relative ischemia of the gravid uterus, and the placental origin of eclampsia. *Am. J. Obstet. Gynecol.* 37:291–293.

Peleg, D., C.M. Kennedy, and S.K. Hunter. 1998. Intrauterine growth restriction: identification and management. *Am. Fam. Physician.* 58:453–460: 466–467.

Peraçoli, J.C., M.V. Rudge, and M.T. Peraçoli. 2007. Tumor necrosis factor-alpha in gestation and puerperium of women with gestational hypertension and pre-eclampsia. *Am. J. Reprod. Immunol.* 57:177–185. http://dx.doi.org/10.1111/j.1600-0897.2006.00455.x

Pijnenborg, R., J.M. Bland, W.B. Robertson, and I. Brosens. 1983. Uteroplacental arterial changes related to interstitial trophoblast migration in early human pregnancy. *Placenta.* 4:397–413. http://dx.doi.org/10.1016/S0143-4004(83)80043-5

Pijnenborg, R., L. Vercruysse, and M. Hanssens. 2006. The uterine spiral arteries in human pregnancy: facts and controversies. *Placenta.* 27:939–958. http://dx.doi.org/10.1016/j.placenta.2005.12.006

Redman, C.W.G. 1991. Current topic: pre-eclampsia and the placenta. *Placenta.* 12:301–308. http://dx.doi.org/10.1016/0143-4004(91)90339-H

Redman, C.W.G., and M. Jefferies. 1988. Revised definition of pre-eclampsia. *Lancet.* 1:809–812. http://dx.doi.org/10.1016/S0140-6736(88)91667-4

Redman, C.W., G.P. Sacks, and I.L. Sargent. 1999. Preeclampsia: an excessive maternal inflammatory response to pregnancy. *Am. J. Obstet. Gynecol.* 180:499–506. http://dx.doi.org/10.1016/S0002-9378(99)70239-5

Reister, F., H.G. Frank, W. Heyl, G. Kosanke, B. Huppertz, W. Schröder, P. Kaufmann, and W. Rath. 1999. The distribution of macrophages in spiral arteries of the placental bed in pre-eclampsia differs from that in healthy patients. *Placenta.* 20:229–233. http://dx.doi.org/10.1053/plac.1998.0373

Reister, F., H.G. Frank, J.C. Kingdom, W. Heyl, P. Kaufmann, W. Rath, and B. Huppertz. 2001. Macrophage-induced apoptosis limits endovascular trophoblast invasion in the uterine wall of preeclamptic women. *Lab. Invest.* 81:1143–1152. http://dx.doi.org/10.1038/labinvest.3780326

Renaud, S.J., L.M. Postovit, S.K. Macdonald-Goodfellow, G.T. McDonald, J.D. Caldwell, and C.H. Graham. 2005. Activated macrophages inhibit human cytotrophoblast invasiveness in vitro. *Biol. Reprod.* 73:237–243. http://dx.doi.org/10.1095/biolreprod.104.038000

Renaud, S.J., S.K. Macdonald-Goodfellow, and C.H. Graham. 2007. Coordinated regulation of human trophoblast invasiveness by macrophages and interleukin 10. *Biol. Reprod.* 76:448–454. http://dx.doi.org/10.1095/biolreprod.106.055376

Renaud, S.J., R. Sullivan, and C.H. Graham. 2009. Tumour necrosis factor alpha stimulates the production of monocyte chemoattractants by extravillous trophoblast cells via differential activation of MAPK pathways. *Placenta.* 30:313–319. http://dx.doi.org/10.1016/j.placenta.2009.01.001

Renaud, S.J., T. Cotechini, J.S. Quirt, S.K. Macdonald-Goodfellow, M. Othman, and C.H. Graham. 2011. Spontaneous pregnancy loss mediated by abnormal maternal inflammation in rats is linked to deficient uteroplacental perfusion. *J. Immunol.* 186:1799–1808. http://dx.doi.org/10.4049/jimmunol.1002679

Rittirsch, D., M.A. Flierl, D.E. Day, B.A. Nadeau, S.R. McGuire, L.M. Hoesel, K. Ipaktchi, F.S. Zetoune, J.V. Sarma, L. Leng, et al. 2008. Acute lung injury induced by lipopolysaccharide is independent of complement activation. *J. Immunol.* 180:7664–7672.

Roberts, J.M., and H.S. Gammill. 2005. Preeclampsia: recent insights. *Hypertension.* 46:1243–1249. http://dx.doi.org/10.1161/01.HYP.0000188408.49896.c5

Roberts, V.H., J. Smith, S.A. McLea, A.B. Heizer, J.L. Richardson, and L. Myatt. 2009. Effect of increasing maternal body mass index on oxidative and nitrative stress in the human placenta. *Placenta.* 30:169–175. http://dx.doi.org/10.1016/j.placenta.2008.11.019

Roggensack, A.M., Y. Zhang, and S.T. Davidge. 1999. Evidence for peroxynitrite formation in the vasculature of women with preeclampsia. *Hypertension.* 33:83–89. http://dx.doi.org/10.1161/01.HYP.33.1.83

Rubin, L.H., K. Witkiewitz, J.S. Andre, and S. Reilly. 2007. Methods for handling missing data in the behavioral neurosciences: don't throw the baby rat out with the bath water. *JUNE.* 5:A71–A77.

Rustveld, L.O., S.F. Kelsey, and R. Sharma. 2008. Association between maternal infections and preeclampsia: a systematic review of epidemiologic studies. *Matern. Child Health J.* 12:223–242. http://dx.doi.org/10.1007/s10995-007-0224-1

Salminen, A., R. Paananen, R. Vuolteenaho, J. Metsola, M. Ojaniemi, H. Autio-Harmainen, and M. Hallman. 2008. Maternal endotoxin-induced preterm birth in mice: fetal responses in toll-like receptors, collectins, and cytokines. *Pediatr. Res.* 63:280–286. http://dx.doi.org/10.1203/PDR.0b013e318163a8b2

Shynlova, O., T. Nedd-Roderique, Y. Li, A. Dorogin, and S.J. Lye. 2013. Myometrial immune cells contribute to term parturition, preterm labour and post-partum involution in mice. *J. Cell. Mol. Med.* 17:90–102. http://dx.doi.org/10.1111/j.1582-4934.2012.01650.x

Smith, G.N., M.C. Walker, and M.J. McGrath. 1999. Randomised, double-blind, placebo controlled pilot study assessing nitroglycerin as a tocolytic. *Br. J. Obstet. Gynaecol.* 106:736–739. http://dx.doi.org/10.1111/j.1471-0528.1999.tb08376.x

Soares, M.J., D. Chakraborty, M.A. Karim Rumi, T. Konno, and S.J. Renaud. 2012. Rat placentation: an experimental model for investigating the hemochorial maternal-fetal interface. *Placenta.* 33:233–243. http://dx.doi.org/10.1016/j.placenta.2011.11.026

Strevens, H., D. Wide-Swensson, A. Grubb, A. Hansen, T. Horn, I. Ingemarsson, S. Larsen, J.R. Nyengaard, O. Torffvit, J. Willner, and S. Olsen. 2003. Serum cystatin C reflects glomerular endotheliosis in normal, hypertensive and pre-eclamptic pregnancies. *BJOG.* 110:825–830. http://dx.doi.org/10.1111/j.1471-0528.2003.02051.x

Szarka, A., J. Rigó Jr., L. Lázár, G. Beko, and A. Molvarec. 2010. Circulating cytokines, chemokines and adhesion molecules in normal pregnancy and preeclampsia determined by multiplex suspension array. *BMC Immunol.* 11:59. http://dx.doi.org/10.1186/1471-2172-11-59

Todt, J.C., Y. Yang, J. Lei, M.R. Lauria, Y. Sorokin, D.B. Cotton, and F.D. Yelian. 1996. Effects of tumor necrosis factor-alpha on human trophoblast cell adhesion and motility. *Am. J. Reprod. Immunol.* 36:65–71. http://dx.doi.org/10.1111/j.1600-0897.1996.tb00141.x

Tosun, M., H. Celik, B. Avci, E. Yavuz, T. Alper, and E. Malatyalioğlu. 2010. Maternal and umbilical serum levels of interleukin-6, interleukin-8, and tumor necrosis factor-alpha in normal pregnancies and in pregnancies complicated by preeclampsia. *J. Matern. Fetal Neonatal Med.* 23:880–886. http://dx.doi.org/10.3109/14767051003774942

Valensise, H., B. Vasapollo, G. Gagliardi, and G.P. Novelli. 2008. Early and late preeclampsia: two different maternal hemodynamic states in the latent phase of the disease. *Hypertension.* 52:873–880. http://dx.doi.org/10.1161/HYPERTENSIONAHA.108.117358

van Asselt, K., S. Gudmundsson, P. Lindqvist, and K. Marsal. 1998. Uterine and umbilical artery velocimetry in pre-eclampsia. *Acta Obstet. Gynecol. Scand.* 77:614–619. http://dx.doi.org/10.1034/j.1600-0412.1998.770607.x

Vatten, L.J., and R. Skjaerven. 2004. Is pre-eclampsia more than one disease? *BJOG.* 111:298–302. http://dx.doi.org/10.1111/j.1471-0528.2004.00071.x

Venegas-Pont, M., M.B. Manigrasso, S.C. Grifoni, B.B. LaMarca, C. Maric, L.C. Racusen, P.H. Glover, A.V. Jones, H.A. Drummond, and M.J. Ryan. 2010. Tumor necrosis factor-alpha antagonist etanercept decreases blood pressure and protects the kidney in a mouse model of systemic lupus erythematosus. *Hypertension.* 56:643–649. http://dx.doi.org/10.1161/HYPERTENSIONAHA.110.157685

Vercruysse, L., S. Caluwaerts, C. Luyten, and R. Pijnenborg. 2006. Interstitial trophoblast invasion in the decidua and mesometrial triangle during the last third of pregnancy in the rat. *Placenta.* 27:22–33. http://dx.doi.org/10.1016/j.placenta.2004.11.004

Viktil, K.K., A. Engeland, and K. Furu. 2012. Outcomes after anti-rheumatic drug use before and during pregnancy: a cohort study among 150,000 pregnant women and expectant fathers. *Scand. J. Rheumatol.* 41:196–201. http://dx.doi.org/10.3109/03009742.2011.626442

Yung, H.W., S. Calabrese, D. Hynx, B.A. Hemmings, I. Cetin, D.S. Charnock-Jones, and G.J. Burton. 2008. Evidence of placental translation inhibition and endoplasmic reticulum stress in the etiology of human intrauterine growth restriction. *Am. J. Pathol.* 173:451–462. http://dx.doi.org/10.2353/ajpath.2008.071193

Zhang, H., Y. Park, J. Wu, Xp. Chen, S. Lee, J. Yang, K.C. Dellsperger, and C. Zhang. 2009. Role of TNF-alpha in vascular dysfunction. *Clin. Sci.* 116:219–230. http://dx.doi.org/10.1042/CS20080196

Zhou, P., X. Luo, H.B. Qi, W.J. Zong, H. Zhang, D.D. Liu, and Q.S. Li. 2012. The expression of pentraxin 3 and tumor necrosis factor-alpha is increased in preeclamptic placental tissue and maternal serum. *Inflamm. Res.* 61:1005–1012. http://dx.doi.org/10.1007/s00011-012-0507-x